Proceedings of the 1992 IEEE
International Conference on Robotics and Automation
Nice, France - May 1992

ROBAT: A Sonar-Based Mobile Robot for Bat-Like Prey Capture

Billur Barshan

Robotics Research Group
Department of Engineering Science
University of Oxford
Oxford, OX1 3PJ U.K.

Roman Kuc

Intelligent Sensors Laboratory
Department of Electrical Engineering
Yale University
New Haven, CT 06520 U.S.A.

Abstract

This paper investigates the prey capture problem in an uncluttered environment for a mobile robot equipped with a wide-beam sonar system. An analytical lower bound for the mean capture time is derived by assuming complete information about the prey. Algorithms using qualitative and quantitative information are implemented for prey capture, and compared in terms of mean capture time and capture probability. Although qualitative information is sufficient, quantitative information assures more efficient prey capture to be achieved over a broader range of system parameters.

1 Introduction

In this paper, the results of the bat-like sonar system in [1] are extended to a mobile robot whose task is to catch a vehicular robot-moth moving along a linear path. The wide-beam sonar system consists of a central transmitter flanked by two receivers. The system is capable of estimating the range r and azimuth θ of an object by extracting the time-of-flight (TOF) information from the detected echo envelopes. Reliable prey localization is feasible over a limited area (the *active region*), defined by the intersection of the sensor directivity patterns. Localization is most accurate when the prey is situated near the center of the beam at nearby ranges where the signal-to-noise ratio (SNR) is large. Because of the analogy of this robotic system to the bat/moth system in nature, we will call our mobile robot $\mathcal{R}$, for ROBAT, and the prey $\mathcal{M}$, for MOTH.

Assuming linear motion of prey allows the problem to be treated both analytically and experimentally. Two measures of success are employed: mean capture time after initial detection (if capture occurs) and probability of capture. In Sec. 2, a lower bound for the mean capture time is derived. Sec. 3 summarizes the different phases of prey capture for our sonar system. Relationship of sensing and control is investigated in Sec. 4, followed by a description of simulation studies in Sec. 5. The results are presented and interpreted in Sec. 6. A description of the robotic system in our laboratory is given in Sec. 7. Experimental results verifying the analysis and the simulations are provided.

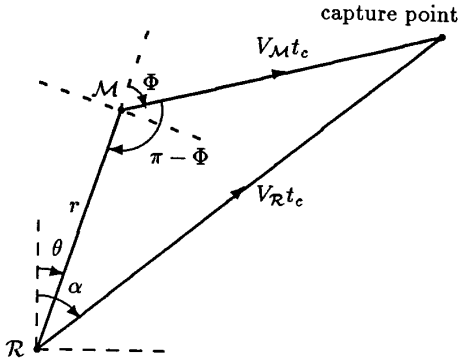

Figure 1: Linearly moving prey.

2 Prey capture with linear motion

We derive a lower bound on the time to capture linearly moving prey, assuming the pursuer has complete knowledge about the evader at all times and points in space. We consider a moth $\mathcal{M}$ moving at speed $V_{\mathcal{M}}$ that is first detected by $\mathcal{R}$ at range r and azimuth θ (Fig. 1). The orientation of $\mathcal{M}$'s linear path, measured with respect to the θ direction, is assumed to be a random variable Φ. With complete information about $\mathcal{M}$, i.e. r, θ, Φ and $V_{\mathcal{M}}$, the $\mathcal{R}$ tends to intercept $\mathcal{M}$ quickly to minimize its energy expenditure [2]. For a given set of parameters, this defines a *unique* linear trajectory with orientation α. From the geometry of Fig. 1, one can solve for α and t_c to get:

$$\alpha = \theta + \sin^{-1}\left[\frac{V_{\mathcal{M}}}{V_{\mathcal{R}}}\sin\Phi\right] \tag{1}$$

$$t_c = \frac{r\left[\frac{V_{\mathcal{M}}}{V_{\mathcal{R}}}\cos\Phi + \sqrt{1-\left(\frac{V_{\mathcal{M}}}{V_{\mathcal{R}}}\right)^2\sin^2\Phi}\right]}{V_{\mathcal{R}}\left[1-\left(\frac{V_{\mathcal{M}}}{V_{\mathcal{R}}}\right)^2\right]} \tag{2}$$

Eq. (2) indicates that prey capture will occur in finite time only if $V_{\mathcal{M}} < V_{\mathcal{R}}$. Capture time is observed to be independent of θ and maximum when $\Phi = 0$. This

0-8186-2720-4/92 $3.00 ©1992 IEEE

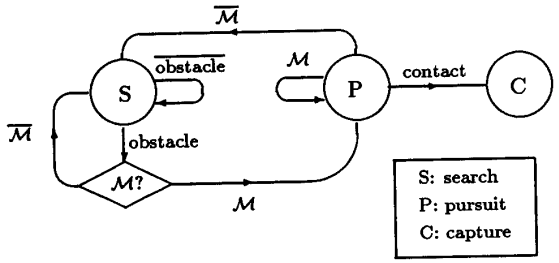

Figure 2: State diagram for the motion of $\mathcal{R}$.

means that moths which flee away directly from the bat in the direction of initial detection take the longest time to capture. We assume that Φ is uniformly distributed in the interval $-\frac{\pi}{2} \leq \Phi \leq \frac{\pi}{2}$. This restriction of Φ limits the cases to $\mathcal{M}$ drifting *away* from $\mathcal{R}$, and eliminates the situation when $\mathcal{M}$ has a velocity component towards $\mathcal{R}$ (suicidal moth!). Taking the expected value of minimum capture time, we get

$$E_\Phi[t_c] = \frac{2r\left[\frac{V_\mathcal{M}}{V_\mathcal{R}} + \mathcal{E}\left(\frac{\pi}{2}, \frac{V_\mathcal{M}}{V_\mathcal{R}}\right)\right]}{\pi V_\mathcal{R}\left[1 - \left(\frac{V_\mathcal{M}}{V_\mathcal{R}}\right)^2\right]} \quad (3)$$

where

$$\mathcal{E}\left(\frac{\pi}{2}, \frac{V_\mathcal{M}}{V_\mathcal{R}}\right) = \int_0^{\frac{\pi}{2}} \sqrt{1 - \left(\frac{V_\mathcal{M}}{V_\mathcal{R}}\right)^2 \sin^2 x}\, dx \quad (4)$$

is the complete elliptic integral of the second kind [3] with $\frac{V_\mathcal{M}}{V_\mathcal{R}} < 1$. This result will be compared to our simulation and experimental results employing information limited by the finite active region and measurement noise (Figs. 4 and 12). Eq. (3) indicates that the mean capture time increases sharply with $V_\mathcal{M}$ and becomes infinite when $V_\mathcal{M}$=$V_\mathcal{R}$. In the ideal case with complete information, capture probability P_c=1. We will find that with the limited information case (which occurs in nature), P_c<1.

3 Phases of prey capture

$\mathcal{R}$'s prey capture strategy consists of three modes analogous to bat foraging behavior [4]. The state diagram is shown in Fig. 2. The initial state is the *search mode* S where $\mathcal{R}$ scans the environment in a stop-and-go pattern at equal time intervals. This type of scan is observed frequently in nature and is called *saltatory search*. At each stop, $\mathcal{R}$ performs a rotation of the sensor system to cover the maximum area possible. The most efficient length for the distance traveled between two scans is related to both the direction of the move and the shape of the volume being searched [5].

When $\mathcal{M}$ is detected, $\mathcal{R}$ switches to *pursuit mode* P. In the pursuit mode, $\mathcal{R}$ moves to reduce the range r and azimuth θ to zero. When r and θ are sufficiently small, $\mathcal{M}$ is considered captured; the process terminates in C. However, $\mathcal{M}$ may move out of the active region after it has been detected (not *all* moths are caught by bats). In this case, $\mathcal{R}$ returns to S, rotating in the direction where $\mathcal{M}$ was last seen.

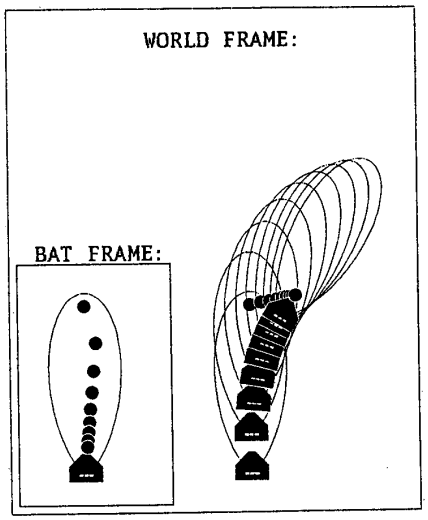

Figure 3: A simulation example.

4 Relationship of sensing and control

This section explores the relationship of sensing and control in robot systems that are to perform a task. Since the measurements of $\mathcal{M}$'s location influence the actions of $\mathcal{R}$, prey capture can be viewed in terms of a control problem [6]. To accomplish prey capture, there are a variety of options [7] for controlling the action of the pursuer $\mathcal{R}$ (and possibly $\mathcal{M}$ for sensory equipped moths, although not considered here). Each option has its own trade-off in performance and complexity. Here, we consider two control strategies for the pursuit mode that use different levels of information. Both methods are memoryless, assume no knowledge of $\mathcal{M}$'s motion, and extract information sequentially from the environment. This means that $\mathcal{R}$'s information about $\mathcal{M}$ is obtained at each scan instant, and consists of noisy measurements of r and θ if $\mathcal{M}$ is within the active region. Hence, the complete knowledge assumption in Sec. 2, used to derive the lower bound on capture time, ceases to be valid.

4.1 Qualitative information

To address the purposive imaging problem [8], the *minimal* information required to achieve prey capture was determined. Successful prey capture by $\mathcal{R}$ that is faster than $\mathcal{M}$ was previously demonstrated by employing the direction θ of $\mathcal{M}$ relative to $\mathcal{R}$ [9, 10]. Our results indicate the binary information that $\mathcal{M}$ is either to the right or left of $\mathcal{R}$'s line-of-sight is sufficient. The ad-hoc nonlinear response by $\mathcal{R}$ is then taken to be a rotation by a fixed angle β to the right or left. This minimum-information/minimum-response strategy is the least sophisticated working method of accomplishing capture that we have investigated.

4.2 Quantitative information

With this strategy, $\mathcal{R}$ moves toward the estimated location of $\mathcal{M}$ within the active region, determined from the most recent echoes which produce a delayed estimate of $\mathcal{M}$'s position, due to the echo travel time. Since range and azimuth can be estimated, $\mathcal{R}$ makes

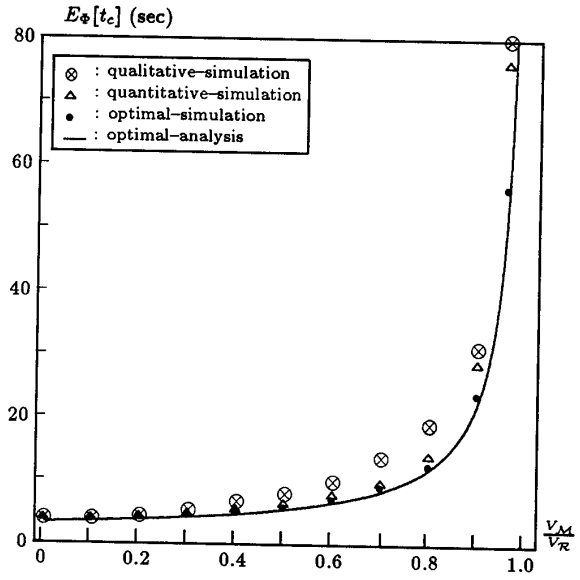

Figure 4: Mean capture time vs. $\frac{V_M}{V_R}$ for V_R=50 cm/s, T_s=1 s, r=200 cm, θ=0°, and β=10°.

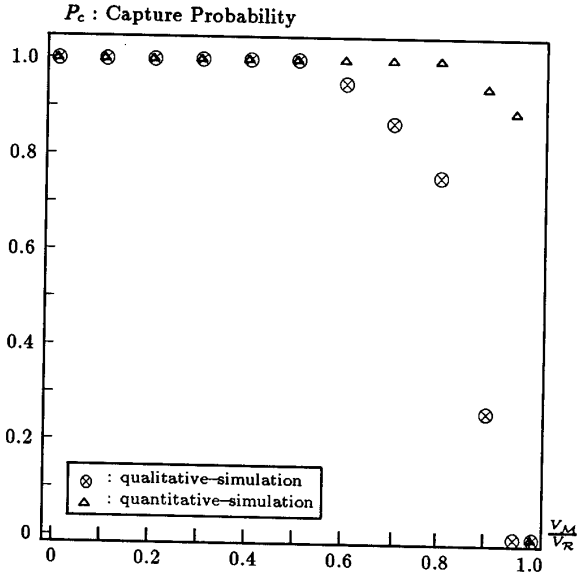

Figure 5: Capture probability vs. $\frac{V_M}{V_R}$ for V_R=50 cm/s, T_s=1 s, r=200 cm, θ=0° and β=10°.

a rotation that centers the beam on $\mathcal{M}$'s current location (to where the moth-meal is located) and steps forward. This way, the accuracy characteristics of the system are exploited [1]. This procedure is repeated several times, updating $\mathcal{M}$'s location after each iteration. This is a more reasonable model given the information available in the bat brain [11]. However, when r is large (distant $\mathcal{M}$), two problems arise. First, the estimates have a large variance since the echo amplitude is comparable to the noise level. Secondly, the TOF is sufficiently long that $\mathcal{M}$ can move a significant distance from its measured location between scans. When r is small, the scan rate is increased by transmitting a new pulse as soon as an echo is received. In this case, this heuristic strategy works well.

5 Simulation studies

To test the significance of the available information, prey capture was simulated by a program that models the physical operation of the actual sonar system on a VAX 3100 work station. Dynamic equations for the motion of the physical robot have been derived and implemented in the simulations.

A simulation example for the quantitative method is shown in Fig. 3. The sonar system is illustrated by a rectangle on $\mathcal{R}$ and its active region is shown in outline. The solid dots represent the sequence of $\mathcal{M}$'s locations. In the bat coordinate system, the relative positions of $\mathcal{M}$ are shown as $\mathcal{R}$ reacts to observations and closes in for capture.

For accurate localization by the sonar system, the simulation is started when $\mathcal{M}$ is located at the edge of $\mathcal{R}$'s active region along θ=0° and starts fleeing at random orientation Φ. For qualitative information, the rotation angle β was chosen to be 10°. When $\mathcal{M}$ escapes out of the active region, for both systems, $\mathcal{R}$ responds by a saltatory search with ±45° rotations that cover the maximum possible area. If $\mathcal{M}$ escapes out of the active region and is not detected within 12 cycles of saltatory search, $\mathcal{M}$ is considered not captured, resulting in a decreased P_c. One hundred realizations are generated to evaluate the penalty incurred on performance when different levels of information are extracted from the sensor system.

6 Performance evaluation results

A quantitative measure of the significance of information is provided by determining the corresponding cost in capture probability and mean capture time for each method. The optimal technique based on complete information yields the highest capture probability and minimum capture time. Penalties incur on performance when suboptimal yet faster techniques are used. The penalty of qualitative systems is not in a significant increase in capture time but rather in a reduced capture probability. The simulation results are shown in Figs. 4–9. From the analysis and verification of our bat-like sonar system, we have observed that three parameters influence prey capture:

6.1 Relative speed $\frac{V_M}{V_R}$

The speed of $\mathcal{M}$ compared to $\mathcal{R}$ is the most important factor in accomplishing prey capture. Mean capture time and capture probability are shown as a function of $\frac{V_M}{V_R}$ in Figs. 4 and 5. As expected, quantitative information yields better performance than qualitative information, but there is a wide range of $\frac{V_M}{V_R}$ values over which they are comparable. The results indicate that moths with velocities below $0.5V_R$ are always captured with both methods. With quantitative information, moths moving as fast as $0.8V_R$ are successfully captured. For $V_M > 0.8V_R$, $\mathcal{M}$ escapes

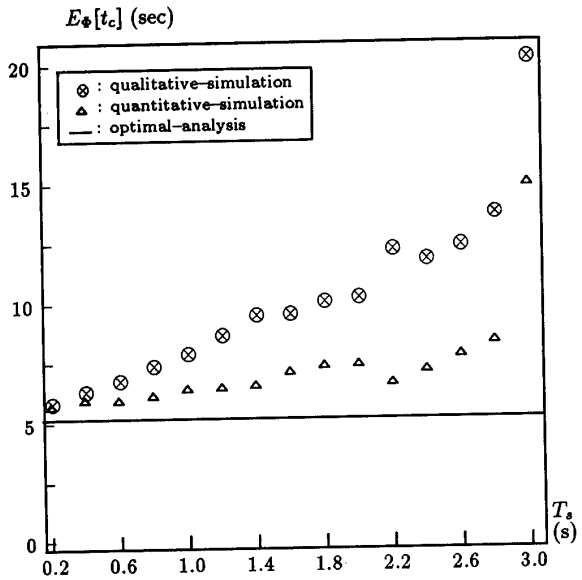

Figure 6: Mean capture time vs. T_s for $V_{\mathcal{R}}$=50 cm/s, $V_{\mathcal{M}}$=25 cm/s, r=200 cm, θ=0° and β=10°.

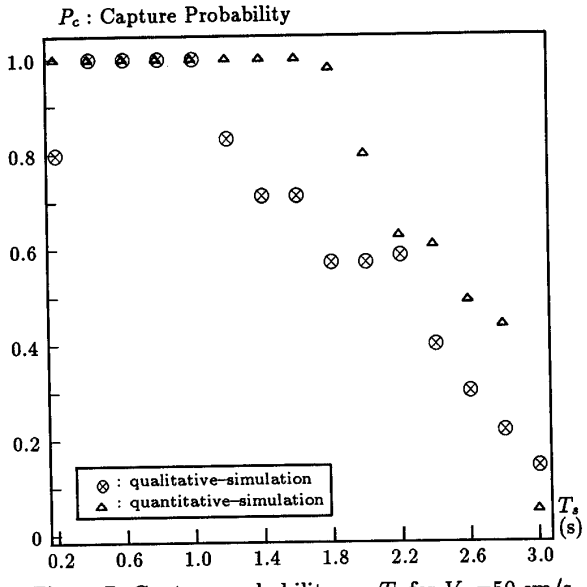

Figure 7: Capture probability vs. T_s for $V_{\mathcal{R}}$=50 cm/s, $V_{\mathcal{M}}$=25 cm/s, r=200 cm, θ=0° and β=10°.

from the active region more often. For the qualitative system, when $V_{\mathcal{M}} > 0.5V_{\mathcal{R}}$, the rotation limited by β allows more moths to escape from the active region.

6.2 Scan interval T_s

In nature, bats transmit a new pulse as soon as the echo from the previous pulse is detected and processed. Then, the scan interval T_s is equal to the TOF measurement plus the processing time of the echoes. When r is large, the TOF is sufficiently long so that $\mathcal{M}$ can move a significant distance from its measured location between two scans. However, a given linear motion of $\mathcal{M}$ corresponds to a larger change in θ at nearby ranges than when $\mathcal{M}$ is distant. Since the beam pattern is also narrower at small r, if the environment is not scanned frequently enough, $\mathcal{M}$ can easily escape the active region. It is to prevent this that bats set their scan interval T_s proportional to range [11], scanning much faster as they approach the prey.

To investigate the effect of the scan interval, T_s was varied by including a hypothetical processing delay in addition to the delay due to TOF. The effect of varying T_s is shown in Figs. 6 and 7. With both methods, a reduction in T_s reduces the phase lag of the control system. The increased phase margin allows more open loop gain in the stable system and, hence, more maneuverability for the bat [12]. Smaller T_s values also create more feedback in the closed-loop system and reduce the effect of localization errors. In this respect, feedback is more important for the qualitative method. Hence, the performance of this method deteriorates very quickly with increasing T_s.

6.3 Effect of β

The performance of the qualitative method for different values of β is shown in Figs. 8 and 9. For these simulations, the saltatory search angle was set equal to β, instead of the constant value of $45OC^o$ used earlier. If β is too extreme the system is over- or underdamped. An overdamped system does not allow $\mathcal{R}$ to follow $\mathcal{M}$, while an underdamped system causes $\mathcal{R}$ to overshoot $\mathcal{M}$. An intermediate value of β=16° yields the highest capture probability and yet reasonably small capture time.

7 Experimental verification

Although the simulations are more flexible and efficient, real robots and the sensor systems are essential to verify the assumptions. Experiments with the robots in our laboratory have indicated results similar to those of the simulations. First, the mobile robot equipped with a wide-beam sonar system is described that detects and captures a simple, randomly moving obstacle in a simple environment. The environment is a 4 m×4 m area free of obstacles other than $\mathcal{M}$.

7.1 Description of ROBAT

A schematic illustration of the robotic system is shown in Fig. 10. The mobile robot $\mathcal{R}$ is a position-controlled vehicle that carries the sonar system onboard with a maximum speed of $V_{\mathcal{R}}$=10 cm/s. It consists of a triangular platform, placed on top of a passive front caster and two stepper motor wheels. The transducers are located high above the platform to eliminate reflections off the platform and the floor. On-board electronics provide excitations for pulse transmission and amplifier/filters for signal detection and envelope extraction. A cable carries the analog signal envelopes to an A/D converter. The control and processing of the signals is accomplished with an IBM PC/XT-286 that extracts information from the sensor data, determines the action to be taken and sends commands to a PDP-11/23 for motor control. Each stepper motor can be driven independently

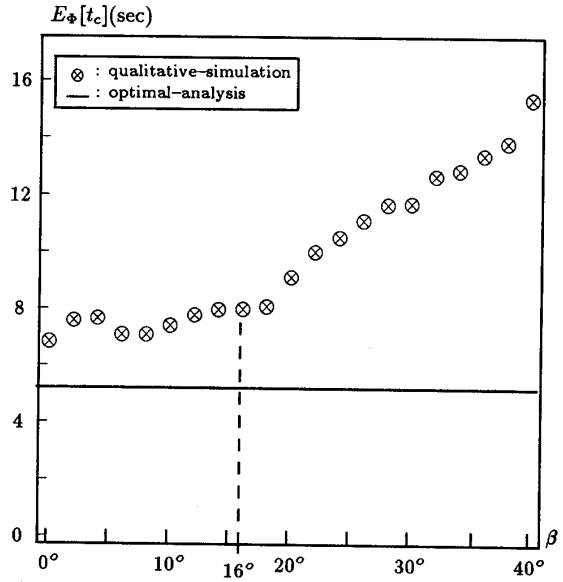

Figure 8: Mean capture time vs. β for $V_{\mathcal{R}}$=50 cm/s and $V_{\mathcal{M}}$=25 cm/s.

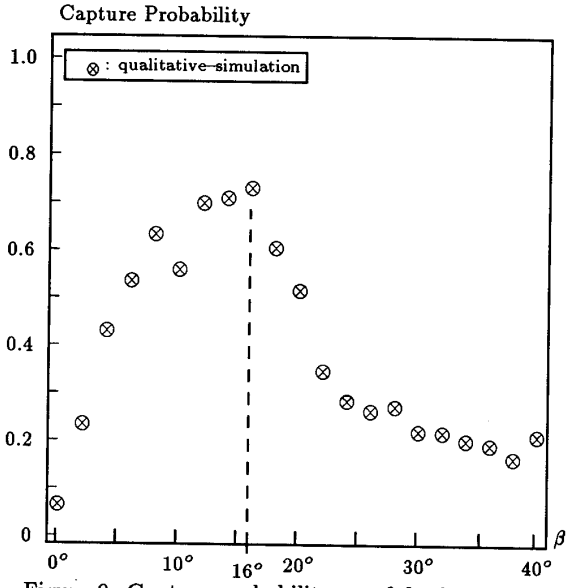

Figure 9: Capture probability vs. β for $V_{\mathcal{R}}$=50 cm/s and $V_{\mathcal{M}}$=25 cm/s.

over a given range of speeds.

7.2 Description of MOTH

Although smaller than $\mathcal{R}$, the second mobile robot $\mathcal{M}$ in our system is similar in that it is a platform driven by two stepper motors. $\mathcal{M}$ carries a vertically-mounted cylinder reflector with diameter 16 cm and height 1 m. Since $\mathcal{M}$ has no sensory feedback, it is *passive prey* , unaware of the presence of $\mathcal{R}$. It is independently controlled through a cable by its own PDP-11/23 to move along a linear trajectory with maximum speed $V_{\mathcal{M}}$=20 cm/s.

7.3 Experimental setup

To verify the analytical results and the comparison of the qualitative and quantitative algorithm performances, experiments were performed in real-time with ROBAT and MOTH. For the following experiments, an average scan interval of T_s=1 s was used as before.

For accurate localization by the sonar system, the experiments are started when $\mathcal{M}$ is located at the center of $\mathcal{R}$'s active region along θ=0° and starts fleeing at random orientation Φ. Algorithms using both qualitative and quantitative information, described in Sec. 4, were implemented on the robotic system. For qualitative information, the rotation angle β was chosen to be 20°. Five different trials were realized for each algorithm at angles Φ=0°, ±30°, ±60°, ±90° for different speeds of $\mathcal{M}$. For a given $V_{\mathcal{M}}$ and Φ, the capture time was averaged over the five trials to compensate for the experimental errors. These errors are due to the low SNR when $\mathcal{M}$ is first detected.

7.4 Experimental results and interpretation

The results for $V_{\mathcal{M}}$= 8,6,4 cm/s are shown in Fig. 11 as a function of Φ. As expected, the experimentally observed capture time decreases with increasing $|\Phi|$, indicating a similar form as the lower bound for capture time. The difference between using qualitative vs. quantitative information is only marginal. However, with the sub-optimal methods, it takes 4–8 s longer to capture the prey. This difference between the experimental results and the minimum capture time increases for faster moths.

Next, the experimental results were averaged over Φ. Since five trials were performed for each of the seven Φ values, the average for a given moth speed is over a total of 35 trials. These results are shown in Fig. 12 as a function of $V_{\mathcal{M}}$. The mean capture time obtained from the qualitative method is only slightly higher than the quantitative information method. On the average, prey capture took 2–4 s longer than minimum capture time.

8 Summary

Two different prey capture strategies were compared for a robotic system, in which a mobile robot equipped with a wide-beam sonar system detects, pursues and captures a second mobile robot with no sensory feedback. Significant parameters for prey capture are the predator prey speed ratio and the scan interval. It was observed that although binary information about the prey direction was sufficient, quantitative information increased the capture probability and reduced the mean capture time. Both systems are comparable when $\frac{V_{\mathcal{M}}}{V_{\mathcal{R}}}$ <0.5. For faster moths, penalty for qualitative information is not a significant increase in capture time, but reduced capture probability.

Acknowledgment

This work was supported by the NSF grant ECS-8802627.

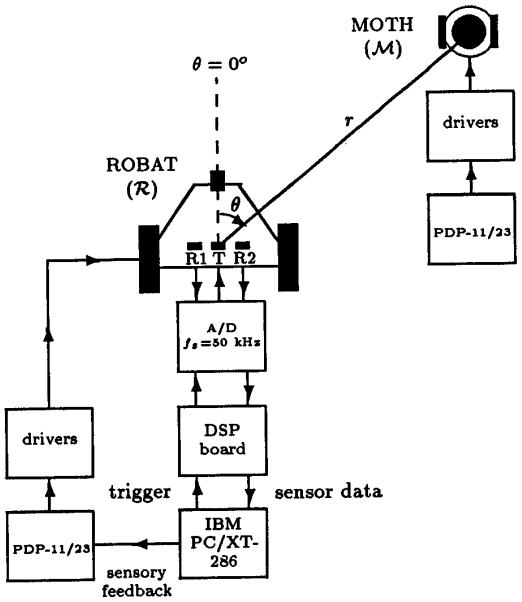

Figure 10: Configuration of the robotic system.

References

[1] B. Barshan and R. Kuc, "A bat-like sonar system for obstacle localization," *IEEE Trans. on Systems, Man and Cybernetics*, 1992. In the press.

[2] J. M. V. Rayner, "The cost of being a bat," *Nature*, vol. 350, pp. 383–384, April 1991.

[3] I. S. Gradshteyn and I. M. Ryzhik, *Table of Integrals, Series and Products*. New York: Academic Press, 1980.

[4] A. Novick, "Acoustic orientation," in *Biology of Bats* (W. A. Wimsatt, ed.), vol. 3, ch. 2, pp. 74–273, New York: Academic Press, 1977.

[5] W. J. O'Brien, H. I. Browman and B. I. Evans, "Search strategies of foraging animals," *American Scientist*, vol. 78, pp. 152–160, March-April 1990.

[6] C.-B. Chang and J. A. Tabaczynski, "Application of state estimation to target tracking," *IEEE Trans. on Automatic Control*, vol. AC-29, pp. 98–109, February 1984.

[7] B. Barshan, *A Sonar-Based Mobile Robot for Bat-Like Prey Capture*. PhD thesis, Yale Univ., 1991.

[8] J. Aloimonos, "Purposive and qualitative active vision," in *Proc. AAAI-90 Workshop on Qualitative Vision*, pp. 1–5, Boston, 1990.

[9] R. Isaacs, *Differential Games*. New York: John Wiley & Sons, 1965.

[10] R. Sharma and J. Aloimonos, "Target pursuit or prey catching using qualitative visual data," in *Proc. AAAI-90 Workshop on Qualitative Vision*, pp. 195–198, Boston, 1990.

[11] N. Suga, "Cortical computational maps for auditory imaging," *Neural Networks*, vol. 3, no. 1, pp. 3–21, 1990.

[12] O. L. R. Jacobs, *Introduction to Control Theory*. Oxford, UK: Oxford Univ. Press, Clarendon Press, 1974.

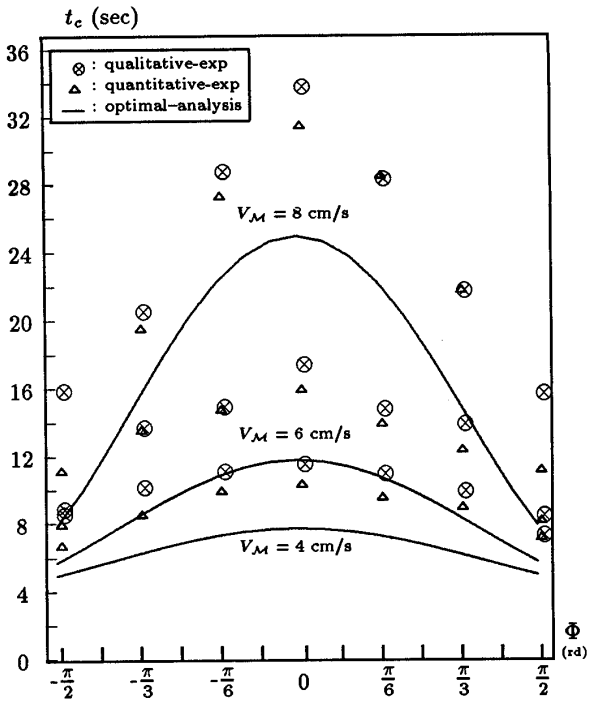

Figure 11: Experimental results showing capture time t_c as a function of Φ for $V_{\mathcal{R}}$=9.8 cm/s and r=80 cm.

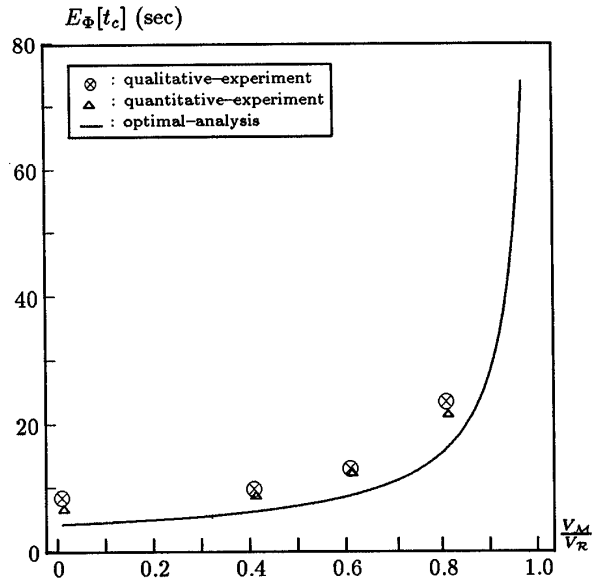

Figure 12: Experimental results showing mean capture time vs. $\frac{V_{\mathcal{M}}}{V_{\mathcal{R}}}$ for $V_{\mathcal{R}}$=9.8 cm/s, T_o=1 s, r=80 cm, θ=0°, and β=20°.